Journal of Hazardous Materials 181 (2010) 27–34

Contents lists available at ScienceDirect

Journal of Hazardous Materials

journal homepage: www.elsevier.com/locate/jhazmat

Rice straw as precursor of activated carbons: Activation with ortho-phosphoric acid

V. Fierro[a,*], G. Muñiz[a,b], A.H. Basta[c], H. El-Saied[c], A. Celzard[a]

[a] Institut Jean Lamour - UMR CNRS 7198, CNRS - Nancy-Université – UPV-Metz, ENSTIB, 27 rue du Merle Blanc, BP 1041, 88051 Epinal Cedex 9, France
[b] Facultad de Ciencias Químicas, Universidad Autónoma de Chihuahua, Circuito Universitario S/N, Chihuahua, Mexico
[c] National Research Centre, Cellulose & Paper Dept., El-Tahrir Street, Dokki-12622, Cairo, Egypt

ARTICLE INFO

Article history:
Received 7 January 2010
Received in revised form 14 April 2010
Accepted 15 April 2010
Available online 21 April 2010

Keywords:
Rice straw
Activated carbon
H_3PO_4
Methylene blue
Adsorption

ABSTRACT

Highly mesoporous activated carbons (ACs) with a mesopore fraction ranging from 42 to 73% were obtained by activation of rice straw (RS) with ortho-phosphoric acid (PA). Due to such a high mesoporosity, these ACs can be successfully used for pollutant removal in aqueous phase. The ACs were prepared at activation temperatures (T) ranging from 350 to 500 °C, using PA to RS weight ratios (R) from 0 to 1.6 and activation times from 0 to 2 h. They were characterised by nitrogen adsorption at −196 °C, SEM-EDX, and methylene blue adsorption. RS is a very heterogeneous material with a variable content of mineral matter: using the product of activated carbon yield multiplied by surface area ($C \times S_{BET}$) as the performance criterion, the best AC was produced at $T = 450$ °C and $R \geq 1$. These conditions lead to S_{BET} higher than 500 $m^2\ g^{-1}$ and a $C \times S_{BET}$ around 270 $m^2\ g^{-1}$.

1. Introduction

Three million tons of rice straws (RS) are produced annually in Egypt. So far, such a resource is mainly considered as a waste, and consequently burnt without any profit, except in a few cases of domestic uses for cooking and heating. Worse, biomass burning is a major source of atmospheric pollution [1], especially through the fumes and the very fine silica particles thus produced, both having a suffocating effect. Although wildfires are prohibited in cultivation fields of most countries, farmers usually keep on burning their crop by-products.

Rice-derived wastes comprise two different materials: husks and straws. Rice husks have been commonly investigated as potential precursors of ACs [2–4]. By contrast, straws have been seldom suggested for this application, whereas other routes of valorisation have been considered in the past, e.g., pulp and paper, construction materials, compost, fuel, production of chemicals such as ethanol and bio-adsorbents [5] and references therein.

To the best knowledge of the present authors, only three works have been carried out using RS as AC precursor, based on chemical activation by potassium hydroxide on one hand [5,6], and by sodium hydroxide on the other hand [7]. In our previous paper [5], three pre-treatment protocols were tested: mechanical, chemical (by NaOH pulping), and a combination of both, followed by a further activation with KOH according to either one or two steps. Employing the combined mechanical–chemical pre-treatment method and a 2-steps KOH activation process, surface areas as high as 1917 $m^2\ g^{-1}$ could be obtained. However, the use of such complex activation protocol working at temperatures as high as 800 °C makes RS-based AC production rather expensive.

Ortho-phosphoric acid (PA), H_3PO_4, is a common activating agent whose use has been extensively reported for preparing activated carbons from agricultural by-products [8–12], wood [13,14], natural [15,16] as well as synthetic [17,18] carbons. PA promotes the bond cleavage in the biopolymers and dehydration at low temperatures [19], followed by extensive cross-linking that binds volatile matter into the carbon product and thus increases the carbon yield. Benaddi et al. [20] showed that the mechanism of PA activation of biomass feedstock occurs through various steps: cellulose depolymerisation, biopolymers dehydration, formation of aromatic rings and elimination of phosphate groups. This allows activated carbons to be prepared with good yields and high surface areas. Activation conditions thus depend on the nature of the precursor, i.e., on the relative amounts of cellulose, hemicellulose, lignin and ashes. For example, the present authors already prepared ACs from lignin (L) by activation with H_3PO_4, and the optimum PA/L weight ratio allowing complete reaction of lignin has been

* Corresponding author. Tel.: +33 329296177; fax: +33 329296177.
E-mail address: Vanessa.Fierro@lcsm-uhp.nancy.fr (V. Fierro).

0304-3894/$ – see front matter © 2010 Elsevier B.V. All rights reserved.
doi:10.1016/j.jhazmat.2010.04.062

Table 1
Activation conditions for RS impregnated with H_3PO_4.

Sample name	Impregnation ratio	Impregnation time (h)	Heating rate (°C min^{-1})	Activation time (h)	Temperature (°C)
R effect (t_a = 2 h and T = 450 °C)					
R000	0	1	5	2	450
R025	0.25	1	5	2	450
R050	0.5	1	5	2	450
R075	0.75	1	5	2	450
Reference	1	1	5	2	450
R120	1.2	1	5	2	450
R140	1.4	1	5	2	450
R160	1.6	1	5	2	450
t_a effect (R = 1 and T = 450 °C)					
AT0	1	1	5	0	450
AT1	1	1	5	1	450
T effect (R = 1 and t_a = 2 h)					
T350	1	1	5	2	350
T375	1	1	5	2	375
T400	1	1	5	2	400
T425	1	1	5	2	425
T475	1	1	5	2	475
T500	1	1	5	2	500

evidenced at a value around 1.0. Further increase of PA/L did not produce changes of weight loss during pyrolysis, and hence no change of carbon yield occurred [21]. From the point of view of porosity development, the optimal PA/L weight ratio was found to range from 1.2 to 1.4, leading to ACs having high surface areas (1300 m^2 g^{-1}) and porosity (0.7 cm^3 g^{-1}) [22].

Given the composition of RS, rich in cellulose and ashes, rather different optimal experimental conditions are thus expected for preparing the best possible adsorbents. The objective of this work was to describe for the first time the properties of RS chemically activated with ortho-phosphoric, and to find the best experimental conditions for obtaining ACs having both with high surface areas and carbon yields.

2. Experimental

2.1. Rice straw characterisation

The contents of α-cellulose, pentosan and lignin have been determined according to methods detailed elsewhere [5]. The average ash content in RS was calculated by weighing a number of samples before and after all the organic matter was burnt by heating in a muffle furnace up to 600 °C (ASTM E1755-01).

2.2. Synthesis of ACs

Rice straw (RS) was impregnated with phosphoric acid (PA) for 1 h using PA to RS weight ratios, *R*, ranging from 0.25 to 1.6. The resultant mixture was introduced in a quartz tube and placed inside a quartz tubular reactor. The latter was placed in a vertical oven, heated at 5 °C min^{-1} up to the final activation temperature, which was held for activation times, t_a, ranging from 0 to 2 h under nitrogen flow. Once the activation was finished, the oven was switched off and the carbonised material let to cool under nitrogen flow. The resultant AC was washed with distilled water in a Soxhlet for 5 days, and then dried overnight in an oven at 105 °C. Table 1 lists the activation conditions and the corresponding name of the ACs thus prepared. The sample synthesised at 450 °C with an activation time of 2 h and a ratio PA/RS of 1 is referred to as the "reference" sample in the following. It is the one to which any other material prepared in different experimental conditions will be compared. According to the nomenclature of Table 1, the reference sample might be also called R100, AT2, or T450.

2.3. Characterisation of ACs

2.3.1. Electron microscopy

The morphology of activated RS samples has been observed by Scanning Electron Microscopy (FEG-SEM Hitachi S 4800) equipped with an EDX (Energy Dispersion of X-rays) instrument. The latter was used for the semi-quantitative analysis of the ashes.

2.3.2. Nitrogen adsorption at −196 °C

The pore texture parameters have been determined from the corresponding nitrogen adsorption–desorption isotherms obtained at −196 °C with an automatic instrument (ASAP 2020, Micromeritics). The samples were previously outgassed at 250 °C for 24 h. The surface areas were determined by the BET calculation method [23] applied to the adsorption branch of the isotherms. The micropore volume, V_{DR}, was calculated according to the Dubinin–Radushkevitch method [24]. The total pore volume, sometimes referred to as the so-called Gurvitch volume, $V_{0.99}$, was defined as the volume of liquid nitrogen corresponding to the amount adsorbed at a relative pressure p/p_0 = 0.99 [25]; the Gurvitch volume is assumed to be the sum micropore + mesopore volumes. The mesopore volume, V_{meso}, was thus calculated as the difference between $V_{0.99}$ and V_{DR}.

2.3.3. Ash content determination

Ash content in ACs was determined in a thermogravimetric device (TAG 1750, Setaram). 20 mg of AC were heated in air according to the following temperature program:

(i) Moisture was measured by the weight loss of the sample heated at 5 °C min^{-1} up to 105 °C, the final temperature being held for 30 min.
(ii) Ash content was next determined on a dry basis by heating the resultant sample at 5 °C min^{-1} from 105 to 650 °C. The latter temperature, chosen according to the D2866-94 ASTM standard (i.e., relevant to activated carbons), was maintained for 60 min.
(iii) Finally, additional heating at 5 °C min^{-1} from 650 to 815 °C was carried out, the latter temperature being maintained for 60 min and now chosen on the basis of the ISO standard 1171 (i.e., corresponding to mineral carbons).

Table 2
Solid yield (i.e., pure activated carbon + ashes), ash content, and textural parameters determined by nitrogen adsorption at −196°C.

Sample name	Solid yield, C (%)	Ash content (%)	S_{BET} ($m^2\,g^{-1}$)	$C \times S_{BET}$ ($m^2\,g^{-1}$)	$V_{0.99}$ ($cm^3\,g^{-1}$)	V_{DR} ($cm^3\,g^{-1}$)	V_{meso} ($cm^3\,g^{-1}$)
R effect (t_a = 2 h and T = 450 °C)							
R000	41.0	41.3	27	11.1	0.04	0.01	0.03
R025	42.2	33.8	359	151.5	0.24	0.14	0.10
R050	35.3	17.4	571	201.4	0.50	0.21	0.29
R075	49.3	36.0	448	220.9	0.41	0.17	0.24
Reference	51.9	33.0	522	270.7	0.55	0.18	0.37
R120	49.9	36.1	540	269.4	0.53	0.19	0.34
R140	45.9	34.5	598	274.0	0.75	0.21	0.54
R160	33.9	16.7	786	266.0	1.05	0.28	0.77
t_a effect (R = 1 and T = 450 °C)							
AT0	34.6	52.6	664	229.8	0.72	0.24	0.48
AT1	44.4	34.1	588	260.9	0.65	0.21	0.44
Reference	51.9	33.0	522	270.7	0.55	0.18	0.37
T effect (R = 1 and t_a = 2 h)							
T350	36.3	20.3	551	200.0	0.57	0.205	0.36
T375	33.9	18.5	576	193.9	0.62	0.213	0.41
T400	39.7	21.4	635	251.9	0.64	0.23	0.41
T425	37.5	27.9	685	257.0	0.75	0.25	0.50
Reference	51.9	33.0	522	270.7	0.55	0.18	0.37
T475	53.2	53.3	378	201.0	0.45	0.14	0.31
T500	39.4	28.5	466	183.70	0.57	0.17	0.39

2.3.4. Methylene blue adsorption

Methylene blue (MB) adsorption is frequently used to test the adsorption performances of ACs [26–28]. Five different amounts of dry powdered AC (typically from 0.05 to 0.5 g) were added to 25 mL of MB of concentration 0.6 g L^{-1} in distilled water. The suspensions were kept in a shaker at a fixed temperature of 30 °C during 24 h. According to a number of previous trials, such a time is enough for guaranteeing adsorption equilibrium of MB over AC surface. The AC suspensions were next filtered, and the residual MB contained in the solution was quantified by UV–vis spectrometry (Lambda 3B UV–vis Spectrophotometer, Perkin Elmer) working at a fixed wavelength of 625 nm. Freundlich and Langmuir equations were applied to the adsorption data at equilibrium. The main difference between these two equations concerns the way the heat of adsorption decreases with surface coverage: Langmuir assumes no decrease, whereas Freundlich assumes a logarithmic decrease. Freundlich's equation [29] reads:

$$q_e = k_f C_e^{1/n} \quad (1)$$

where q_e is the amount of MB adsorbed per unit mass of adsorbent (mg g^{-1}), k_f is Freundlich's constant related to the adsorption capacity (mg g^{-1}·(mg L^{-1})^n), C_e is the equilibrium concentration of adsorbate in the solution (mg L^{-1}), and n is the empirical parameter representing the energetic heterogeneity of the adsorption sites (dimensionless).

Langmuir's equation [30] can be written as:

$$\frac{C_e}{q_e} = \frac{1}{Q_0\beta} + \frac{C_e}{Q_0} \quad (2)$$

where C_e and q_e have the same meaning as before; Q_0 is the maximum uptake per unit mass of adsorbent (mg g^{-1}), and β is Langmuir's constant related to the adsorption energy (L mg^{-1}). The efficiency of the adsorption process can be predicted by the dimensionless equilibrium parameter E_L, which is defined by the following equation:

$$E_L = \frac{1}{1 + \beta C_0} \quad (3)$$

where C_0 is the initial concentration of methylene blue in the solution (mg L^{-1}). The adsorption is considered as irreversible when $E_L = 0$, favourable when $0 < E_L < 1$, linear when $E_L = 1$, and unfavourable when $E_L > 1$.

3. Results

3.1. Rice straw characterisation

Raw rice straw (RS) has very high ash content (mainly silica) of 18.2%, on average, much higher than in any other kind of cereal straw. Given that heat-treatment unavoidably induces the release of volatiles, the fraction of ashes in the final activated carbon is expected to be even higher. α-Cellulose, pentosan and Klason lignin contents are found to be 51.3, 12.7 and 17.8%, respectively. It is well known that such components have different carbon yields, typically 20% for cellulose and even below for hemicellulose, and 40% for lignin. The fraction of lignin being lower than 20%, rather low carbon yields are foreseen, even in PA activation hinders the formation of volatiles and thereby leads to higher yields than what is obtained by simple pyrolysis at the same temperature (see below).

3.2. Activated carbon yield and textural properties

Table 2 presents the yield (C) of as-prepared activated carbon and the corresponding ash content, as well as some physical parameters determined by nitrogen adsorption at −196 °C such as S_{BET}, $V_{0.99}$, V_{DR} and V_{meso}. The product $C \times S_{BET}$ is also given. By "yield of as-prepared activated carbon", we mean the weight ratio of final to initial solid, i.e., including the ashes. The true carbon yield, i.e., only taking into account the carbon present inside the solid, is thus lower. No difference in ash content could be experimentally found, whatever the final temperature used for burning the organic matter (see Section 2.3.3). Thus, heating at 815 °C instead of 650 °C just allowed checking our results.

The ash content is strongly modified through chemical activation, indeed varying in a very wide range of values: from 16.7 to 53.3% (see 3rd column of Table 2), without any logical correlation with the synthesis parameters. Each line of Table 2 represents the data for one given sample (in other words, not averages of a set of values), consequently such high differences may be ascribed to significant heterogeneity in the composition of rice straw. By contrast, in the figures of the present manuscript, several different samples have been tested for giving one's idea about the scattering of the results. The assumption of heterogeneity of composition is strongly supported as soon as the results are analysed on the basis

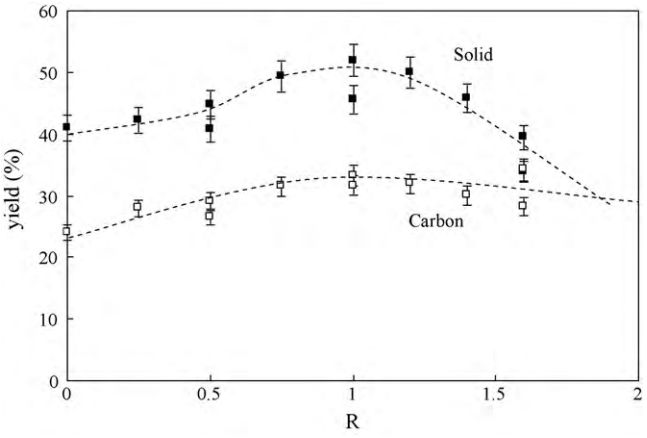

Fig. 1. Effect of the impregnation ratio on solid (i.e., activated carbon + ashes) and carbon (i.e., without ashes) yields (t_a = 2 h and T = 450 °C).

of either total solid (i.e., whole, as-prepared, activated carbon, thus comprising pure carbon + ashes) or carbon alone. Removing the contribution of the ashes from the weight of as-prepared activated carbons, the true carbon yield and other specific properties can be deduced. In some of the following figures, the results are thus presented for both as-obtained and pure activated carbons (i.e., with and without ashes, respectively). Such double representations shed light on the activation mechanism of RS.

3.2.1. Effect of the impregnation ratio

As a first example, Fig. 1 shows the dependence of both solid yield (i.e., the as-prepared activated carbon: full symbols) and pure carbon yield (empty symbols) on the impregnation ratio, R. The solid yield presents an uneven curve having a maximum at approximately 50% for R = 1. By contrast, the changes of carbon yield are much lower, increasingly slowly up to R = 1, then being roughly constant within the uncertainties of the measurements. Such trends may be explained on the basis of both activation conditions and ash contents. As suggested in Section 1, phosphate and polyphosphate bridges are created when PA reacts with RS, increasing the carbon yield through the hindrance of volatilisation. The carbon yield is thus seen to increase by typically 10% when the amount of PA increases from R = 0 to R = 1. However, beyond a critical value of R, here close to 1, no additional organic matter is able to react with PA. Therefore, adding more phosphoric acid has no effect on the carbon yield that cannot further increase. The excess of PA thus also reacts with the ashes (mainly silica), leading to the formation of silico-phosphates and other salts. Several compositions and structures are possible for silico-phosphates, e.g., SiP_2O_7, $Si_5O(PO_4)_6$, or $Si(HPO_4)_2$, H_2O [31], some of them being soluble in water. These compounds are extracted by boiling water in the Soxhlet wherein the activated carbons are washed, thus decreasing the solid yield. The ash content is thus seen to vary between 41% for RS carbonised without H_3PO_4 to 33% and 17% at R = 1 and R = 1.6, respectively (see Table 2).

Fig. 2 presents SEM pictures of R120 AC at different magnifications. Activation does not modify the morphology of the original particles, and the structure of the vegetal cells is fully maintained. Observation at the highest magnification revealed that the outer surface of RS is covered with small silico-phosphate crystals, whose qualitative composition was indeed revealed by EDX analysis.

Fig. 3a shows the effect of the impregnation ratio on the specific surface area, S_{BET}, which was again calculated on the basis of either total solid (full symbols) or pure activated carbon (empty symbols). Obviously, the surface area is the lowest in the absence of activating agent (R = 0), and quickly increases as soon as R > 0. As far as the total solid is concerned, S_{BET} values are stable, around 520 $m^2\ g^{-1}$, for R ranging from 0.5 to 1.2. Then, the surface area increases gradually for $R \geq 1.2$ due to the progressive consumption of ashes by the excess of PA. Assuming that only the carbonaceous part of the material provides surface area, the corresponding S_{BET} can be calculated from the (pure) carbon yield. This assumption is quite realistic, given the following calculation. After heat-treatment, silica grains are not expected to be smaller than 100 nm. Assuming a spherical shape and a density of 2.2 for silica particles, and a density of 1.8 for carbon, a silica content as high as 50 wt.% of the total solid would lead to an additional surface area of 14 $m^2\ g^{-1}$, much lower than the BET values reported in Table 2. The BET surface area of pyrolysed (non-activated) RS is, however, of the same order of magnitude of the aforementioned calculation, thereby supporting its relevance. The contribution of pure activated carbon to the global surface area of the solid is thus seen to increase monotonously with R in Fig. 3a, leading to S_{BET} = 940 $m^2\ g^{-1}$ for R = 1.6. Such a monotonous increase of (pure) carbon surface area is readily explained by the opening and development of the porosity, due to simultaneous activation and progressive elimination of silico-phosphates.

Fig. 3b shows the evolution with R of nitrogen adsorption–desorption isotherms at −196 °C. At low relative

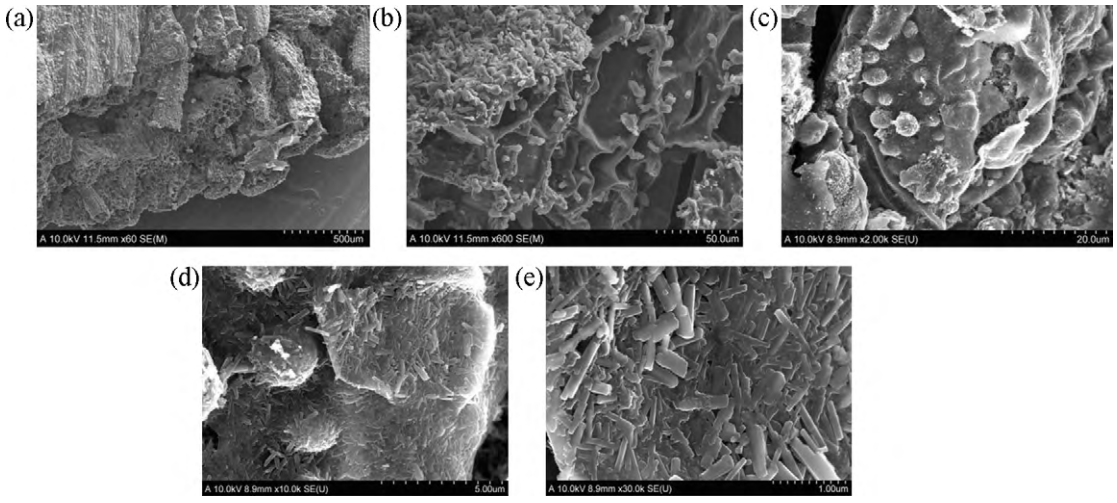

Fig. 2. SEM pictures of ACs prepared from RS activated with phosphoric acid (R = 1.2, T = 450 °C, t_a = 2 h) at different magnifications: (a) 45×; (b) 400×; (c) 2000×; (d) 10,000×; (e) 30,000×.

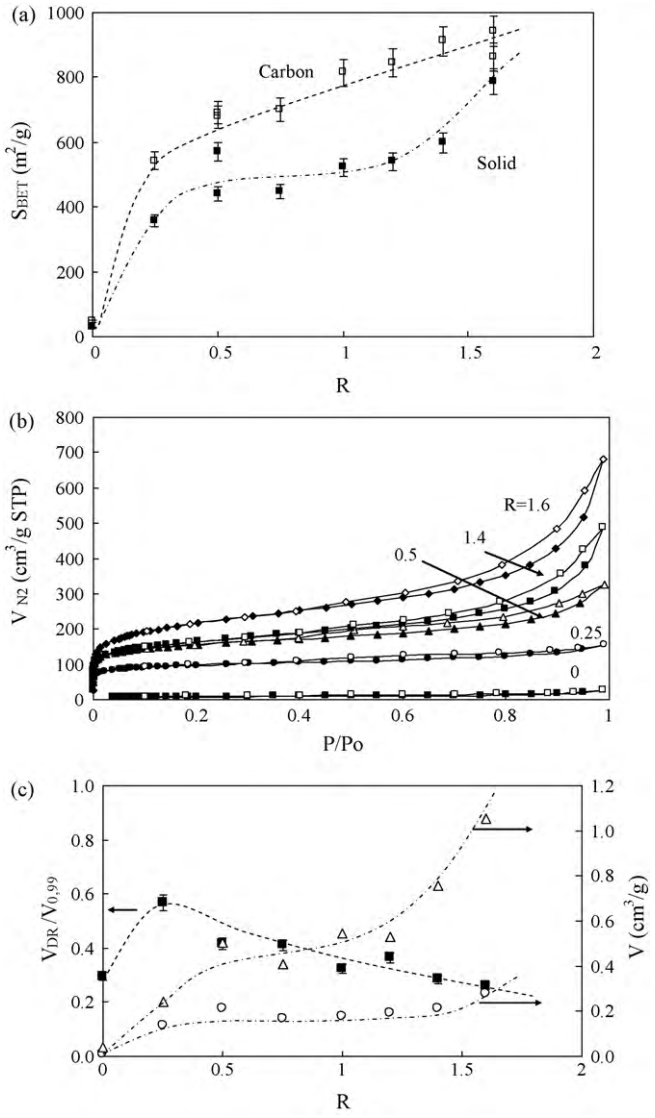

Fig. 3. Effect of the impregnation ratio on: (a) BET surface area basing on either total solid (full symbols) or pure activated carbon (empty symbols); (b) nitrogen adsorption (full symbols) and desorption (empty symbols) isotherms; (c) micropore (circles) and total pore volumes (triangles) on one hand, and micropore fraction (full squares) on the other hand, all based on total solid (t_a = 2 h and T = 450 °C).

pressures, all the ACs except the one without PA (i.e., corresponding to pyrolysed, non-activated, RS) present a sharp increase in the N_2 uptake due to the existence of micropores. As R increases, the elbow of the isotherms widens, evidencing the broadening of the micropore size distribution. The slopes of the plateaus increase as well, and the hysteresis loops are increasingly enlarged. The latter findings are related to the development of mesoporosity.

Deduced from Fig. 3b, Fig. 3c shows the effect of impregnation ratio, R, on total and micropore volumes on one hand, and on the micropore fraction on the other hand, defined as the ratio $V_{DR}/V_{0.99}$. These pore volumes are those of the as-produced solid: carbon + ashes. However, given the aforementioned postulation about the contribution of ashes to surface area, the pore volumes reported here most probably also correspond to those of the pure carbonaceous matter. V_{DR} and $V_{0.99}$ both increase steadily with R, though V_{DR} tends to stabilise from R = 0.5 to R = 1.5. Since the total pore volume continuously increases, so does the mesopore volume. The ratio $V_{DR}/V_{0.99}$ consequently shows a maximum, at an impregnation ratio as low as R = 0.25. The action of PA on RS thus essentially leads to mesoporous activated carbons. For example, the reference sample (R = 1) is 67% mesoporous. It seems that microporosity can further develop only after the ashes that may block the pores are removed with high amounts of phosphoric acid, i.e., at impregnation ratios higher than 1.5 (see Fig. 3c).

3.2.2. Effect of the activation time

Fig. 4a and b shows the evolution with activation time, t_a, of yields and surface areas, respectively, at the same impregnation ratio R = 1. The reference sample corresponds to t_a = 2 h. Increasing the PA/RS contact time spent in the furnace leads to higher yields and correspondingly lower surface areas. This finding can be understood on the basis of concurrent depolymerisation of cellulose and lignin by H_3PO_4 and cross-linking of the resultant fragments into a carbonaceous solid, according to the mechanism claimed in Section 1. The first step leads to oligomers that can be extracted by washing in the Soxhlet, giving lower yields at short activation times. At higher activation times, cross-linking occurs, so more solid material is recovered at the end of the heat-treatment. Such a phenomenon was already observed for activation of lignin with NaOH, but was considered as insignificant [32]; in the present case, the increase of solid and carbon yields with activation time is clear and not negligible. As seen in Fig. 4a, at least 2 h seem to be required for getting the maximum (pure) carbon yield, lower times leading to incomplete (cross-linking) reaction.

According to the aforementioned mechanism of activated carbon formation, a material with more open porosity is obtained at low activation time. Increasing the latter thus decrease the BET surface area, as observed in Fig. 4b. An additional mechanism is the blocking of pores by ashes. At activation time zero (i.e., the PA/RS mixture is heated up to 450 °C and then immediately cooled), the ashes are in the form of fine, well dispersed particles, that tend to gather at higher activation times. With such a mechanism, more porosity is blocked at high activation time, explaining why the surface area of the pure carbon decreases faster with activation time than that of the total solid.

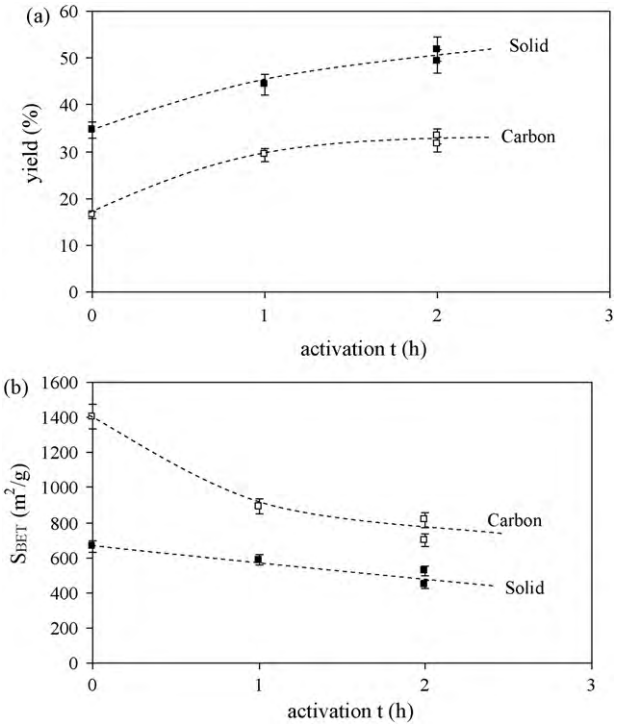

Fig. 4. Effect of activation time on: (a) solid and carbon yields; (b) surface areas of solid and carbon (R = 1 and T = 450 °C).

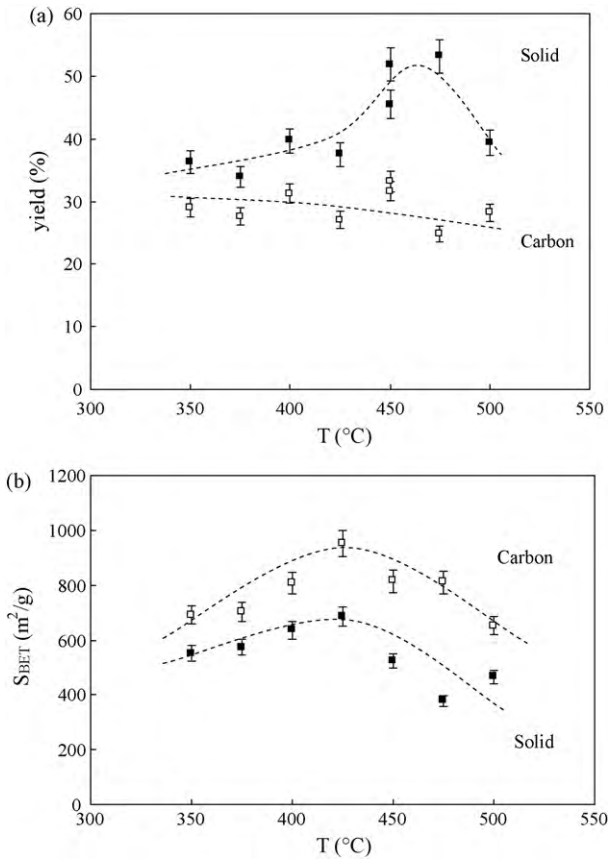

Fig. 5. Effect of activation temperature on: (a) solid and carbon yields; (b) surface areas of solid and carbon ($R = 1$; $t_a = 2$ h).

The reference sample is thus the one having the lowest surface area but the highest yield. Its $C \times S_{BET}$ product is higher than that obtained with other activation times, and thus represents a good compromise.

3.2.3. Effect of the activation temperature

The influence of synthesis temperature, T, is presented in Fig. 5. As seen in Fig. 5a, an unexpected maximum yield of total solid is reached between 450 and 475 °C. However, once the contribution of the ash content is subtracted, the obtained carbon yield decreases slightly, and understandably, with activation temperature. The aforementioned maximum solid yield is thus due to the strong heterogeneity of the raw material. As far as the authors know, it is the first time that pure carbon and total solid are separated like this, and shown to behave so differently. The low decrease of carbon yield as a function of synthesis temperature was also reported for lignin activated with PA [22], and is ascribed to the improved activation process, leading to higher porosity and thereby to lower amounts of resultant solid.

The surface areas of both as-prepared solids and pure activated carbons are plotted in Fig. 5b as a function of T. A maximum is always obtained at 425 °C, for which S_{BET} values of 685 and 950 $m^2\,g^{-1}$ are obtained for solid and carbon, respectively (i.e., only slightly higher than those corresponding to the reference sample: $T = 450$ °C). This behaviour is qualitatively the same as the one observed with lignin activation with ortho-phosphoric acid [22], for which the highest surface areas were obtained at 600 °C. Finding optimal surface areas at a much lower temperature for rice straw should be related to its composition, i.e., to the existence of cellulose and hemicelluloses that degrade at lower temperatures than lignin. 450 °C is indeed a rather usual temperature for the activation of biomass (namely, comprising lignin associated to cellulose and hemicellulose). Examples of references have been given in Section 1. The observed maximum is the result of pore development and pore widening, both favoured by temperature, and leading to two antagonistic contributions on surface area: formation of microporosity and formation of mesoporosity. The former increases the surface area through the formation of narrow pores, whereas the latter decreases it through the formation of increasingly wider pores. Too wide pores become macropores, almost not contributing to the surface area. The resultant effect of both pore creation and pore widening is a maximum observed in the total micropore + mesopore volume at a synthesis temperature of 425 °C, as seen in the 6th column of Table 2. Such a maximum matches the one observed for BET surface area.

3.3. Methylene blue adsorption

The adsorption behaviour of the RS-derived activated carbons has been studied by evaluating the removal efficiency of methylene blue (MB) according to the conditions detailed in Section 2. MB, a rather big, heterocyclic, dye molecule soluble in water, is a good choice for testing adsorbents whose mesoporosity suggests their application for pollutant adsorption in liquid phase. MB, having the formula $(C_{16}H_{18}N_3S)^+$, Cl^- once dissolved in water indeed possesses a molecular size of 0.7 nm × 1.6 nm based on Van der Waals radii [33]; the hydrated form is expected to be even bigger, thus having affinity for carbon mesopores possessing an aromatic nature.

Table 3 gathers Freundlich and Langmuir parameters for MB removal, obtained by fitting Eqs. (1) and (2), respectively, to the adsorption data of nine selected activated carbons. Langmuir's model better fits the experimental data than does Freundlich's model, given that the corresponding correlation coefficient of the former, R^2, was found to be most of times equal to 1.00. Adsorption is usually considered as satisfactory when Freundlich's constant n takes values within the range 1–10. n was lower than 10 for all the ACs tested, suggesting good adsorption properties. The values of Q_0, β, E_L and R^2, derived from application of Langmuir's model, are also listed in Table 3. The values of E_L are always lower than 1 for all the ACs, the lowest ones indicating a more favourable behaviour toward MB adsorption. The values of maximum uptake, Q_0, are found to vary from 21.4 mg g^{-1}, for the non-activated material (i.e., RS just pyrolysed at 450 °C), up to values around 110 mg g^{-1} for the ACs prepared at the highest temperatures with an impregnation ratio of 1. The reference material is among the ones leading to the highest maximum uptake Q_0. Table 3 shows that activation temperature and activation time have a rather low effect on the adsorption properties, as far as the values of Q_0 are compared. By contrast, the impregnation ratio has a major influence, and values of R lower than 1 lead to poor adsorbents. These findings are obviously related to the changes of pore texture already discussed above. However, the magnitude of their impact on the adsorption performance is hardly predicted, hence the importance of having carried out these experiments.

Fig. 6a shows the relationship between Q_0 and S_{BET} for ACs prepared from RS by H_3PO_4 activation (present study) and those prepared by KOH activation [5]. The present ACs exhibit a limit Q_0 close to 110 mg g^{-1}, much lower than the values reached by KOH-activated carbons (up to 529 mg g^{-1}). This finding is due to the corresponding lower surface areas and pore volumes of materials prepared with phosphoric acid. However, as emphasised in Section 1, the present ACs are much cheaper to produce. Therefore, their comparatively lower performances should be easily compensated by using higher amounts in water treatment. In the case of KOH-activated rice straw, the maximum uptake was directly proportional to the surface area in the whole range of S_{BET} studied:

Table 3
Freundlich and Langmuir parameters for MB removal by ACs prepared from H_3PO_4 activation of raw rice straw under different activation conditions.

	Freundlich			Langmuir			
	k_f (mg g^{-1})(mg L^{-1})^n	n	R^2	Q_0 (mg g^{-1})	β (L mg^{-1})	$E_L \times 100$	R^2
R000	5.08	3.04	0.96	21.38	0.023	6.76	0.98
R025	20.27	1.00	0.92	87.72	4.4×10^{-4}	78.89	0.93
R075	25.29	4.72	0.90	88.65	0.063	2.58	0.97
Reference	1.02	6.19	0.99	109.11	0.232	0.71	1.00
AT0	34.70	4.94	0.92	91.32	0.411	0.40	1.00
T350	56.98	7.12	0.80	103.20	7.02	0.02	1.00
T375	26.19	4.02	0.89	101.01	0.08	2.04	0.95
T400	47.09	5.22	0.80	110.38	0.88	0.19	1.00
T500	1.40	1.15	0.87	111.48	0.398	0.42	1.00

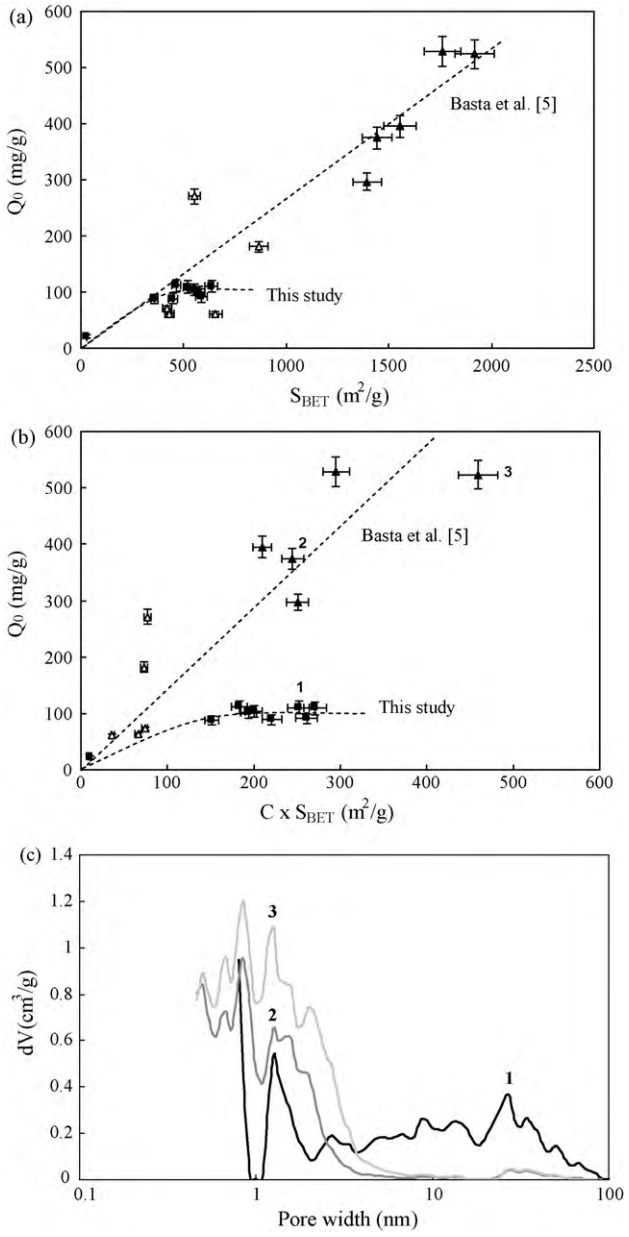

Fig. 6. Maximum MB uptake at equilibrium (30 °C) as a function of (a) BET surface area, and (b) product of solid yield by surface area, of ACs prepared from RS: in the present study using phosphoric acid (full squares), and in the work of Basta et al. [5] using potassium hydroxide (1-step process: empty triangles and 2-steps process: full triangles). (c) Pore size distribution of the AC samples #1, #2 and #3 indicated in (b).

from 420 to 1917 m^2 g^{-1}. Such a linear relationship is not so well followed by H_3PO_4-derived ACs, suggesting that their pore size distribution is not so suitable (too broad and centred on too wide pore sizes) for adsorbing efficiency of the dye molecule.

From a practical and economical point of view, as important as the surface area, S_{BET}, is the material yield, C. Table 2 gives the values of the product $C \times S_{BET}$ for ACs prepared from RS activated by H_3PO_4, ranging from 152 to 274 m^2 g^{-1}. ACs prepared by 1-step and 2-steps KOH activation processes led to values of $C \times S_{BET}$ within the ranges 36–74 and 210–451 m^2 g^{-1}, respectively [5]. Because of the rather high solid yield, compared to that obtained with activation by KOH, the present product $C \times S_{BET}$ therefore takes intermediary values. Fig. 6b shows the relationship between Q_0 and $C \times S_{BET}$ for the same ACs as in Fig. 6a. Again, a linear correlation is found for ACs made by KOH activation, whether the process had one (empty symbols) or two steps (full symbols). Such linear relationship is not observed for ACs prepared by H_3PO_4 activation except, maybe, at low $C \times S_{BET}$ values. Above 150 m^2 g^{-1}, the maximum adsorption uptake Q_0 saturates near 100 mg g^{-1}. This finding suggests that, whatever the activation condition, RS heat-treated with PA is not able to lead to better adsorbents. The synthesis parameters should thus uppermost be chosen for obtaining the highest yield. This very important conclusion makes the reference material among the best compromise for being used in water treatment.

Fig. 6c shows the pore size distribution (PSD) of three selected ACs referred to as #1, #2 and #3 in both Fig. 6b and d. These materials have been chosen for comparison because of the following reasons: #1 and #2 are ACs presenting the same value of the product $C \times S_{BET}$, i.e., around 250 m^2 g^{-1}, but have been prepared by activation with H_3PO_4 and KOH, respectively. #3 is the best AC obtained in Basta et al. [5], having a $C \times S_{BET}$ equal to 459 m^2 g^{-1}. Despite having nearly the same value of $C \times S_{BET}$, samples #1 and #2 present very different PSDs: on one hand, #2 is only 30% mesoporous and most of this porosity is narrower than 5 nm; on the other hand, #1 is 64% mesoporous, and most of its mesopores are wider than 5 nm. Finally, #3 has a much higher surface area (1917 m^2 g^{-1}) than #2 (1444 m^2 g^{-1}), but the PSDs are qualitatively similar.

The pore size distributions given in Fig. 6c account for the observed adsorption properties, and support all the aforementioned statements about them. As evidenced by the PSD of #1, a too broad porosity has indeed no effect on the adsorption performances. Increasing the amount of such porosity through supplementary activation is thereby useless, and explains why the values of Q_0 saturate. Pores having the suitable width, below 5 nm in the present case, present superior adsorption performances. #2 is thus much better than #1 from that point of view, as evidenced in Fig. 6b. Finally, increasing the pore volume without significant broadening of the porosity further improves the adsorption properties, explaining why #3 is even better than #2. In the case of RS activation with PA, it is not possible to develop the porosity without broadening it at the same time. Therefore, adsorption performances will be definitely limited.

It should be stressed that the production of PA-derived ACs is far less expensive than that of better materials obtained by 2-steps KOH activation. The present process based on H_3PO_4 indeed comprises only one single step process achieved at a temperature as low as 450 °C, and which could probably be also carried out under self-generated atmosphere, i.e., without any continuous flow of inert gas. Therefore, H_3PO_4 activation has unquestionable interest compared to KOH activation, even if the performances of the resultant adsorbents are comparatively lower. Because of their low cost, it should not be a problem for using PA-derived adsorbents in higher amounts for reaching adsorption uptakes of more expensive materials.

4. Conclusion

The first systematic study for preparing ACs by chemical activation of RS with PA has been carried out. Separating the contributions of ashes and carbon allowed explaining unexpected behaviours that were ascribed to heterogeneity of raw RS composition. Besides, the own properties of pure carbon could be determined. The experimental conditions: $T = 450\,^{\circ}C$, $t_a = 2$ h, $R = 1$, are a good compromise for getting a correct carbon yield $\times$ S_{BET} product. The highest possible adsorption performances were indeed obtained with this reference material. Modifying the synthesis parameters only broadens the porosity, and therefore do not improve the adsorption properties.

Acknowledgements

The financial support of the Egyptian Academy of Sciences and the French Ministry of Foreign Affairs in the framework of the Imhotep Program is thanked. The authors also gratefully acknowledge the financial support of the CPER 2007–2013 "Structuration du Pole de Competitivité Fibres Grand'Est" (Competitiveness Fibre Cluster), through local (Conseil Général des Vosges), regional (Region Lorraine), national (DRRT and FNADT) and European (FEDER) funds.

References

[1] J.J. Lee, G. Engling, S.C.C. Lung, K.Y. Lee, Particle-size characteristics of levoglucosan in ambient aerosols from rice straw burning, Atmos. Environ. 42 (2008) 8300–8308.
[2] N. Yalçin, V. Sevinç, Studies of the surface area and porosity of activated carbons prepared from rice husks, Carbon 38 (2000) 1943–1945.
[3] Y. Guo, K. Yu, Z. Wang, H. Xu, Effects of activation conditions on preparation of porous carbon from rice husk, Carbon 41 (2000) 1645–1687.
[4] G.T.K. Fey, C.L. Chen, High-capacity carbons for lithium–ion batteries prepared from rice husk, J. Power Sources 97–98 (2001) 47–51.
[5] A.H. Basta, V. Fierro, H. El-Saied, A. Celzard, 2-Steps KOH activation of rice straw: an efficient method for preparing high-performance activated carbons, Bioresour. Technol. 100 (2009) 3941–3947.
[6] G.H. Oh, C.R. Park, Preparation and characterization of rice straw based porous carbons with high adsorption capacity, Fuel 81 (2002) 327–336.
[7] E. Schroder, K. Thomauske, C. Weber, A. Hornung, V. Tumiatti, Experiments on the generation of activated carbon from biomass, J. Anal. Appl. Pyrol. 79 (2007) 106–111.
[8] B.S. Girgis, A.A. El-Hendawy, Porosity development in activated carbons obtained from date pits under chemical activation with phosphoric acid, Micropor. Mesopor. Mater. 52 (2002) 105–117.
[9] T. Vernersson, P.R. Bonelli, E.G. Cerrella, A.L. Cukierman, *Arundo donax* cane as a precursor for activated carbons preparation by phosphoric acid activation, Bioresour. Technol. 83 (2002) 95–104.
[10] J. Guo, A.C. Lua, Adsorption of sulphur dioxide onto activated carbon prepared from oil-palm shells with and without pre-impregnation, Sep. Purif. Technol. 30 (2003) 265–273.
[11] R.A. Shawabkeh, D.A. Rockstraw, R.K. Bhada, Copper and strontium adsorption by a novel carbon material manufactured from pecan shells, Carbon 40 (2002) 781–786.
[12] Y. Diao, W.P. Walawender, L.T. Fan, Activated carbons prepared from phosphoric acid activation of grain sorghum, Bioresour. Technol. 81 (2002) 45–52.
[13] H. Benaddi, T.J. Bandosz, J. Jagiello, J.A. Schwarz, J.N. Rouzaud, D. Legras, F. Béguin, Surface functionality and porosity of activated carbons obtained from chemical activation of wood, Carbon 38 (2000) 669–674.
[14] M. Jagtoyen, F. Derbyshire, Activated carbons from yellow poplar and white oak by H_3PO_4 activation, Carbon 36 (1998) 1085–1097.
[15] C. Toles, S. Rimmer, J.C. Hower, Production of activated carbons from a Washington lignite using phosphoric acid activation, Carbon 34 (1996) 1419–1426.
[16] H. Teng, T.S. Yeh, L.Y. Hsu, Preparation of activated carbon from bituminous coal with phosphoric acid activation, Carbon 36 (1998) 1387–1398.
[17] A.M. Puziy, O.I. Poddubnaya, B. Gawdzik, M. Sobiesiak, D. Dziadko, Heterogeneity of synthetic carbons obtained from polyimides, Appl. Surf. Sci. 196 (2002) 89–97.
[18] A.M. Puziy, O.I. Poddubnaya, A. Martínez-Alonso, F. Suárez-García, J.M.D. Tascón, Characterization of synthetic carbons activated with phosphoric acid, Appl. Surf. Sci. 200 (2002) 196–202.
[19] M. Jagtoyen, F. Derbyshire, Some considerations of the origins of porosity in carbons from chemically activated wood, Carbon 31 (1993) 1185–1192.
[20] H. Benaddi, D. Legras, J.N. Rouzaud, F. Béguin, Influence of the atmosphere in the chemical activation of wood by phosphoric acid, Carbon 36 (1998) 306–309.
[21] V. Fierro, V. Torné-Fernández, D. Montané, A. Celzard, Study of the decomposition of kraft lignin impregnated with orthophosphoric acid, Thermochim. Acta 433 (2005) 142–148.
[22] V. Fierro, V. Torné-Fernández, A. Celzard, Kraft lignin as a precursor for microporous activated carbons prepared by impregnation with ortho-phosphoric acid: synthesis and textural characterisation, Micropor. Mesopor. Mater. 92 (2006) 243–250.
[23] S. Brunauer, P.H. Emmet, E. Teller, Adsorption of gases in multimolecular layers, J. Am. Chem. Soc. 60 (1938) 309–319.
[24] M.M. Dubinin, Fundamentals of the theory of adsorption in micropores of carbon adsorbents—characteristics of their adsorption properties and microporous structures, Carbon 27 (1989) 457–467.
[25] S.J. Gregg, K.S.W. Sing, Adsorption, Surface Area and Porosity, 2nd ed., Academic Press, London, 1982.
[26] V. Torné-Fernández, J.M. Mateo-Sanz, D. Montané, V. Fierro, Statistical optimization of the synthesis of highly microporous carbons by chemical activation of Kraft Lignin with NaOH, J. Chem. Eng. Data 54 (2009) 2216–2221.
[27] L.C.A. Oliveira, E.I. Pereira, K. Sapag, M.C. Pereira, Preparation of activated carbon from coffee husks utilizing $FeCl_3$ and $ZnCl_2$ as activating agents, J. Hazard. Mater. 165 (2009) 87–94.
[28] F. Raposo, M.A. De La Rubia, R. Borja, Methylene blue number as useful indicator to evaluate the adsorptive capacity of granular activated carbon in batch mode: influence of adsorbate/adsorbent mass ratio and particle size, J. Hazard. Mater. 165 (2009) 291–299.
[29] H. Freundlich, Ueber die adsorption in loesungen, Z. Phys. Chem. 57 (1907) 385–470.
[30] I. Langmuir, The adsorption of gases on plane surfaces of glass, mica and platinum, J. Am. Chem. Soc. 40 (1918) 1361–1368.
[31] C. Coelho, F. Babonneau, T. Azaïs, L. Bonhomme-Coury, J. Maquet, G. Laurent, C. Bonhomme, Chemical bonding in silicophosphate gels: contribution of dipolar and J-derived solid state NMR techniques, J. Sol–Gel Sci. Technol. 40 (2006) 181–189.
[32] V. Fierro, V. Torné-Fernández, A. Celzard, Methodical study of the chemical activation of Kraft lignin with KOH and NaOH, Micropor. Mesopor. Mater. 101 (2007) 419–431.
[33] P. Simoncic, T. Armbruster, Cationic methylene blue incorporated into zeolite mordenite-Na: a single crystal X-ray study, Micropor. Mesopor. Mater. 81 (2005) 87–95.